



# A new procedure for the determination of 21 macro- and trace elements in human fetal urine using an inductively coupled plasma mass spectrometry with dynamic reaction cell (ICP-DRG-MS) equipped with a micro-flow nebulizer

Adam Sajnog<sup>a,b,\*</sup>, Marcin Tkaczyk<sup>c</sup>, Małgorzata Stańczyk<sup>c</sup>, Krzysztof Szaflik<sup>d</sup>,  
Joanna Suliburska<sup>e</sup>, Rafał Kocyłowski<sup>f</sup>, Danuta Barańkiewicz<sup>a</sup>

<sup>a</sup> Department of Trace Analysis, Faculty of Chemistry, Adam Mickiewicz University, Poznań, ul. Uniwersytetu Poznańskiego 8, 61–614, Poznań, Poland

<sup>b</sup> Center for Advanced Technology, Adam Mickiewicz University, Poznań, ul. Uniwersytetu Poznańskiego 10, 61–614, Poznań, Poland

<sup>c</sup> Department of Pediatrics, Immunology and Nephrology, Polish Mother's Memorial Hospital Research Institute, ul. Rzgowska 281/289, 93–338, Łódź, Poland

<sup>d</sup> Department of Gynecology, Fertility and Fetal Therapy, Polish Mother's Memorial Hospital Research Institute, ul. Rzgowska 281/289, 93–338, Łódź, Poland

<sup>e</sup> Institute of Human Nutrition and Dietetics, Poznan University of Life Sciences, ul. Wojska Polskiego 31, 60–624, Poznań, Poland

<sup>f</sup> PreMediCare New Med Medical Center, ul. Drużbickiego 13, 61–693, Poznań, Poland

## ARTICLE INFO

**Keywords:**  
ICP-MS  
Micro-flow nebulizer  
Human fetal urine  
Elements  
Procedure development  
Metrology

## ABSTRACT

The procedure for determination of 21 macro- and trace elements – Li, Na, Mg, Al, K, Ca, V, Cr, Mn, Fe, Co, Cu, Zn, Se, Sr, As, Cd, Sb, Ba, Pb and U – in human fetal urine by inductively coupled plasma mass spectrometry (ICP-MS) was developed and validated. The application of a micro-nebulizer and a dynamic reaction cell (DRC) allowed to perform a full analysis of small volumes (200 µL) of urine collected from human fetuses without the need for sample digestion with closed microwave systems. The procedure and ICP-MS instrument was thoroughly optimized in order to reliably determine both macroelements and ultra-trace concentrations of elements. The internal standard method (Ge, Rh and Tb) was applied in order to encompass signal drift and non-spectral interferences. The rules of metrology were used in order to ensure the quality of the results: (1) the procedure was validated, (2) the uncertainty of the measurement results was estimated and (3) the traceability of the measurement result was established by using the certified reference material with matching matrix (Seronorm Trace Elements Urine L-1). Also, the analyte addition method to the artificial urine was employed for additional confirmation of trueness of the procedure. The selected parameters of the procedure were as follows: (a) limits of detection – (0.00023–53 µg L<sup>-1</sup>) for U and Ca, respectively, (b) recoveries of the reference value – 81%–136% for Mn and Cd, respectively (c) linearity expressed as R – greater than 0.999, and (d) expanded relative uncertainties (k = 2) – 13%–66% for Sr and Cd, respectively. The developed and validated procedure was applied to 58 samples of urine collected from human fetuses. The samples were diluted with nitric acid and analyzed without further treatment. The procedure allowed to reliably determine both macro- and trace elements in very low volume of sample in a single analytical run.

## 1. Introduction

Chemical elements have a significant impact on the developing human fetus. The source of the minerals available for fetus is the umbilical cord and amniotic fluid. The composition of the umbilical cord blood and amniotic fluid is dependent on the mother's diet, lifestyle and

environmental factors. For the proper development of fetus, the amount and composition of amniotic fluid is controlled by the tissues of amniotic sac. The fluid is constantly circulating in the sac and is also ingested and “inhaled” by the fetus, and is absorbed in the intestines and lungs, but the reabsorption of the fluid components takes place in the amnion and chorion [1]. Moreover, the fetus, after developing the kidneys, urinates

\* Corresponding author. Department of Trace Analysis, Faculty of Chemistry, Adam Mickiewicz University, Poznań, ul. Uniwersytetu Poznańskiego 8, 61–614, Poznań, Poland.

E-mail address: [adam.sajnog@amu.edu.pl](mailto:adam.sajnog@amu.edu.pl) (A. Sajnog).

<https://doi.org/10.1016/j.talanta.2020.121672>

Received 1 July 2020; Received in revised form 10 September 2020; Accepted 14 September 2020

Available online 17 September 2020

0039-9140/© 2020 Elsevier B.V. All rights reserved.

directly to the amniotic fluid which may be then recirculated and filtered by the mother's tissues in the womb. The volume of the urine produced by the fetus depends on the gestation week and approximately is  $4.2 \text{ mL h}^{-1}$  in fetuses of 20 weeks and  $52.2 \text{ mL h}^{-1}$  of 40 weeks of gestation [2]. The mineral composition of the urine provides useful information about the health of the organism, the exposure to the toxic elements and renal function. Although, it must be noted that the mineral composition of urine may change significantly due to the organism's hydration, the part of the day, the inhomogeneity of the urine (first versus mid-stream), taken medications or physical exercise [3]. Urine is composed in approximately 94% of water, and the rest are organic and mineral components which are excreted by the kidneys, mainly urea, sodium, potassium, chlorides, ammonia, inorganic phosphates and sulfates, creatinine, uric acid and others [4].

The accurate analysis of content of chemical elements in urine is very important for the medical diagnosis, therefore, the reliable analytical procedure must be developed and validated. Various instrumental techniques are employed for the elemental analysis of urine, which differ in the means of the sensitivity, selectivity, detection limits, sample volume, automatization and required staff qualification. For the determination of mineral content in urine the analytical techniques must be sensitive to chemical elements, therefore, the techniques based on atomic spectroscopy are used, for example: atomic absorption spectrometry (AAS) [5], cold vapor AAS (CVAAS) for mercury determination [6], graphite furnace AAS (GFAAS) [7] and inductively coupled plasma optical emission spectrometry (ICP-OES) [8]. More recently, the techniques based on mass spectrometry are increasingly used due to their multielemental capabilities, excellent detection limits and interference removal features, like high resolution mass analyzers and reaction/collision cells, namely inductively coupled plasma mass spectrometry (ICP-MS) [9]. The hyphenation of ICP-MS with chromatographs allow to on-line separation of chemical species of elements, for example species of variable toxicity of arsenic, mercury, antimony or selenium [10,11]. Application of laser ablation ICP-MS enables to analyze dried spots of urine on paper or plastic base prepared from  $1 \mu\text{L}$  to  $300 \mu\text{L}$  urine droplets without the need for additional sample preparation, digestion or using chemicals [12,13].

The aim of this study was to develop and validate a new procedure for determination of macro- and trace elements in human fetal urine by ICP-MS equipped with a direct reaction cell (DRC) and a micro-flow nebulizer. The developed procedure allows to analyze 21 elements, including macro- and trace elements, in small volumes of urine in 3 modes of ICP-MS operation (DRC/standard) in a single analytical run. The developed procedure was thoroughly validated and the traceability of the measurement results was established with stated uncertainty.

## 2. Material and methods

The study was accepted by the Local Ethics Committee of Polish Mother's Memorial Hospital Research Institute (No:1/2016) and conducted according to the Declaration of Helsinki. All the pregnant women, and later parents and guardians of the neonates gave informed consents for participation in the study.

### 2.1. Chemical and reagents

An ultrapure Milli-Q water (Direct-Q 3 UV, Merck, Darmstadt, Germany) and concentrated nitric acid (Suprapur, Merck, Darmstadt, Germany) was used in the study for all samples, blanks and standards in order to obtain 1% acid concentration. A multielemental stock solution, containing 30 elements at the concentration of  $10 \text{ mg L}^{-1}$  in 5% nitric acid (Multi-element Calibration Standard 3, PerkinElmer, Shelton, CT, USA) and single element stock solutions for Ca, K, Mg and Na with concentrations  $10,000 \text{ mg L}^{-1}$  (PerkinElmer, Shelton, CT, USA) were used for calibration standards and method validation. The instrument performance was optimized on a daily basis with the Smart Tune

Solution – ELAN DRC/PLUS/II (PerkinElmer, Shelton, CT, USA). A solution of 1% nitric acid served as a blank sample for calibration and 3% nitric acid was used as a washing solution between samples for 30 s. A calibration curve was generated based on the standard solutions of elements in 1% nitric acid with the concentrations: ( $0.1\text{--}100 \mu\text{g L}^{-1}$ ) for Al, As, Ba, Be, Cd, Co, Cr, Cu, Fe, Li, Mn, Pb, Sb, Se, Sr, U, V, Zn; ( $100\text{--}50,000 \mu\text{g L}^{-1}$ ) for Ca, Mg; ( $100\text{--}300,000 \mu\text{g L}^{-1}$ ) for K, Na. The stock solutions of Sc, Ge, Rh and Tb with concentrations of  $1000 \text{ mg L}^{-1}$  (PerkinElmer, Shelton, CT, USA) were used for preparation of internal standard (ISTD) solution with the concentration  $10 \mu\text{g L}^{-1}$  in 1% nitric acid. The salts and organic compounds were used for artificial urine: sodium chloride (Suprapur,  $\geq 99.99\%$ , Merck, Darmstadt, Germany), potassium chloride (Suprapur,  $\geq 99.999\%$ , Merck, Darmstadt, Germany), creatinine (for biochemistry,  $\geq 99.0\%$ , Merck, Darmstadt, Germany), urea (for biochemistry,  $\geq 99.5\%$ , Merck, Darmstadt, Germany), ammonium phosphate monobasic (trace metals basis,  $\geq 99.99\%$ , Merck, Darmstadt, Germany) and sodium sulfate (Emsure,  $\geq 99.0\%$ , Merck, Darmstadt, Germany).

### 2.2. Sample collection

Inclusion criteria to the study were:

1. Obstructive uropathy by ultrasound with megabladder detected in at least 2 separate examination with or without hydronephrosis with normal or reduced amniotic fluid volume
2. Singleton pregnancy
3. Patient consent for prenatal intervention

Fetuses with multiple genetic abnormalities and/or abnormal karyotype were excluded from further evaluation.

Study group characteristics. All the patients diagnosed with Lower Urinary Tract Obstruction (LUTO) were offered a prenatal intervention of vesico-amniotic shunting (VAS) and a prenatal and postnatal follow-up in the reference center. Preoperatively, a detailed ultrasound examination (Voluson E8, GE Healthcare) was carried out to confirm the diagnosis of obstructive uropathy and exclude any other major defects. Obstructive uropathy was diagnosed by the presence of enlarged bladder (megabladder) with or without "keyhole" sign. A diagnostic "keyhole" sign is seen in PUV, indicating continuity between distended bladder and the dilated posterior urethra proximal to the valves. Changes in renal parenchyma – increased echogenicity or structure and cyst formation were also described. Oligohydramnios was defined by single deepest pocket of less than 2 cm.

Vesico-amniotic shunting procedure. Ultrasound scanning was used to obtain a transverse section of the enlarged bladder and define the appropriate site of entry on the maternal abdomen which was infiltrated with local anesthetic (10 mL of 1% lignocaine) down to the myometrium. Under continuous ultrasound guidance, the shunt (diameter 2 mm, length 12 cm; Rocket KCH Fetal Bladder Catheter, Washington, United Kingdom) was inserted.

58 samples of urine were collected into polypropylene (PP) 2 mL Eppendorf vials within several months and stored in  $-20^\circ\text{C}$ . The frozen samples were thawed in room temperature just before the analysis. 200  $\mu\text{L}$  of urine was transferred by the automatic pipette to 15 mL PP metal-free centrifuge tubes (VWR, PA, USA), and 30  $\mu\text{L}$  of 65%  $\text{HNO}_3$  was added, followed by 1770  $\mu\text{L}$  of Milli-Q water.

### 2.3. Instrumentation

The measurements were performed on a quadrupole ICP-MS, model ELAN DRC II (PerkinElmer SCIEX, Toronto, Canada) with 99.999% argon (Linde, Kraków, Poland) as plasma, auxiliary and sample gas. The instrument was equipped with a glass cyclonic Cinnabar spray chamber with a volume of 20 mL (PerkinElmer, Waltham, MA, USA) and a glass concentric micro-uptake nebulizer MicroMist with  $0.1 \text{ mL min}^{-1}$  sample

flow (PerkinElmer, Waltham, MA, USA). The PVC sample tubing (PerkinElmer, Waltham, MA, USA) with internal diameter of 0.25 mm and 0.19 mm were used for sample and ISTD solution uptake respectively. The sample and ISTD tubing were connected to the T-connector before the spray chamber. The speed of peristaltic pump was change to 17 RPM from standard 20 RPM which improved signal stability without the loss of intensity. The measurements were performed in three modes, including with the DRC, in the single analytical run for all standards and samples: standard, DRC with 99.999% ammonia (Linde Gaz Polska, Kraków, Poland) and DRC with 99.999% oxygen (Linde Gaz Polska, Kraków, Poland). The analytical method included 21 elements, both macro- and trace elements: Li, Na, Mg, Al, K, Ca, V, Cr, Mn, Fe, Co, Cu, Zn, Se, Sr, As, Cd, Sb, Ba, Pb and U. The operating conditions for ICP-MS are listed in Table 1.

#### 2.4. Certified reference materials (CRM)

A CRM with the matrix matched to the analyzed samples of fetal urine, Seronorm Trace Elements Urine L1 (Sero, Billingstad, Norway) with certified concentrations of analyzed elements, was applied in order to establish the traceability of the measurement results and to validate the analytical procedure. Additional non-matrix matched CRMs – SLRS-6 River Water (NRC Canada, Ottawa, Canada) and TM-24.4 fortified diluted lake Ontario water (NRC Canada, Ottawa, Canada) – were applied for validation of the analytical procedure.

#### 2.5. Software

ICP-MS measurement were performed with the dedicated PerkinElmer software Elan ver. 4.3. All operations on analytical data were performed with Microsoft Excel 2016. Corel PaintShop Pro 2019 was used for graphical processing of figures.

### 3. Results and discussion

The application of micronebulizer with low sample uptake was crucial for the analysis of fetal urine due to the limited sample volume, which varied in the range of 200  $\mu\text{L}$ –1000  $\mu\text{L}$ . Therefore, in order to completely analyze all collected samples, the micronebulizer and low volume spray chamber were applied. Low volume chamber allows for a faster sample wash-in and wash-out times, signal stabilization and good sensitivity in comparison to the standard cyclonic chamber of approximately 50 mL volume, which is preferable and beneficial for low sample

**Table 1**  
Operating conditions of ICP-MS.

Instrument	PerkinElmer Sciex ELAN 6100 DRC II
Nebulizer/spray chamber	MicroMist 0.1 mL min <sup>-1</sup> /20 mL Cyclonic Cinnabar
Nebulizer gas flow (L/min)	1.0
Auxiliary gas flow (L/min)	1.2
Plasma gas flow (L/min)	16
RF Power (W)	1400
Peristaltic pump speed (RPM)	17
Lens setting	Autolens calibrated
Detector mode	Dual (pulse counting and analog mode)
Dwell time (ms)	50
DRC gas flow rate (mL min <sup>-1</sup> )	ammonia: 0.3; oxygen: 0.5
RPq	ammonia: <sup>27</sup> Al 0.35; <sup>51</sup> V 0.3; <sup>52</sup> Cr 0.4; <sup>55</sup> Mn 0.7; <sup>56</sup> Fe 0.6; <sup>63</sup> Cu 0.6; <sup>64</sup> Zn 0.5 oxygen: <sup>82</sup> Se 0.2; <sup>91</sup> As 0.5
RPa	standard: <sup>23</sup> Na 0.019; <sup>26</sup> Mg 0.015; <sup>39</sup> K 0.019; <sup>43</sup> Ca 0.015
Sweeps	10
Replicates	3

uptake using the micronebulizer. The application of micronebulizer with approximately 0.1 mL min<sup>-1</sup> sample flow rate allowed obtaining the parameters, such as sensitivity, precision, oxide and double ions ratios, on similar level as with the standard glass concentric nebulizer with approximately 0.9 mL min<sup>-1</sup> sample flow rate. However, due to the significantly better nebulization efficiency of the micronebulizer, the sample uptake is reduced by a factor of approximately 5, which allowed to perform the multielemental analysis with a little sample volume using three DRC modes. The analysis time was roughly 5 min, including the wash-in and wash-out times and stabilization of DRC gas flow.

#### 3.1. Optimization of DRC

Atoms that are present in a sample matrix are subjected to highly energetic conditions, when passing through plasma, which make them prone to form polyatomic species. Those newly formed polyatomic ions with m/z (mass to charge ratio) equal to the analyzed isotopes will result in artificially higher signals of analytes, which is called spectral interferences [14]. Both standard mode and DRC modes with oxygen and ammonia gasses were employed and evaluated in order to minimize the influence of polyatomic spectral interferences. The gas flow and rejection parameters of the corresponding parameters in Mathieu equation q (RPq) and a (RPa) were optimized for selected elements: As and Se in oxygen mode, and Al, V, Cr, Mn, Fe, Cu and Zn in ammonia mode. The most prominent polyatomic interferences for measured isotopes are presented in Table S1 in Supplementary material [15]. Oxygen was found to be the most effective in reduction of polyatomic interferences for As and Se. In the case of As, the analyzed m/z was 91 which corresponds to the thermodynamically stable polyatomic ion, <sup>75</sup>As<sup>16</sup>O<sup>+</sup>, as a result of the chemical reaction of As and O in the cell. Measurement of <sup>75</sup>As<sup>16</sup>O<sup>+</sup>, instead of <sup>75</sup>As<sup>+</sup>, provides better sensitivity and lower limits of detection, especially in a chlorine-rich matrix. Ammonia is the most preferable reaction gas in DRC mode for most of the interference-loaded isotopes [16]. The ratios of signals measures in standard and DRC modes in 1% blank are presented in Table 2. The most significant reduction in blank signal, and therefore reduction of spectral interferences, was observed for V and Cr.

The optimization of DRC parameters – DRC gas flow and RPq – were performed so as to obtain high sensitivity of analytical signals, high precision and signal to background ratios. Additionally, in the case of the limited sample volume also the time of analysis is an important factor, so the DRC flow rate must be set to a single value for a given DRC gas in order to avoid switching between multiple gas flow rate settings and time-consuming DRC stabilization. The “DRC method development” feature in the Elan software allowed to measure signal of elements in DRC mode while automatically switching between the desired flow rate of reaction gas and the RPq value. For the DRC optimization, a solution of artificial urine served as a matrix sample. The artificial urine was prepared in Milli-Q water with the following composition: NaCl 1 g L<sup>-1</sup>,

**Table 2**  
Signal ratios for elements measured in standard and DRC mode for a blank sample.

Measured m/z and corresponding isotope	blank signal intensity $\pm$ standard deviation		intensity ratio standard/DRC
	Standard mode (cps)	DRC mode (cps)	
<sup>27</sup> Al	3902 $\pm$ 258	1418 $\pm$ 94	2.8
<sup>51</sup> V	1365 $\pm$ 196	3 $\pm$ 1	488
<sup>52</sup> Cr	3922 $\pm$ 73	58 $\pm$ 5	68
<sup>55</sup> Mn	475 $\pm$ 51	21 $\pm$ 10	23
<sup>56</sup> Fe	41,618 $\pm$ 501	1013 $\pm$ 109	41
<sup>63</sup> Cu	249 $\pm$ 59	190 $\pm$ 56	1.3
<sup>64</sup> Zn	823 $\pm$ 93	436 $\pm$ 87	1.9
<sup>82</sup> Se	2420 $\pm$ 50	339 $\pm$ 56	7.1

KCl 0.25 g L<sup>-1</sup>, creatinine 1 g L<sup>-1</sup>, urea 10 g L<sup>-1</sup>, ammonium phosphate monobasic 0.25 g L<sup>-1</sup> and sodium sulfate 0.5 g L<sup>-1</sup>. Spiked artificial matrix was used in the optimization of DRC and in the trueness assessment. A spiked matrix sample was obtained after addition of 5 µg L<sup>-1</sup> of analytes measured in DRC mode (Al, V, Cr, Mn, Fe, Cu, Zn, As, Se). Both samples, spiked and unspiked artificial matrix, were analyzed, while the parameters of DRC were changing automatically in the range: DRC gas flow rate (0.1–1.0 mL min<sup>-1</sup>) and RPq value (0.05–0.8).

The signals for matrix and spiked matrix samples are then combined and the background equivalent concentration (BEC) is calculated according to the formula

$$BEC = \frac{I_{\text{blank}} \cdot C_{\text{spike}}}{I_{\text{spike}} - I_{\text{blank}}}$$

where  $I_{\text{blank}}$  – intensity of the blank sample,  $I_{\text{spike}}$  – intensity of the spiked blank sample,  $C_{\text{spike}}$  – concentration of the analyte spike [17]. The obtained data is visualized in the graphs in Fig. S.1–S.9 in Supplementary material. The resulting graphs facilitate the selection of a single DRC gas flow rate for all analyzed elements in DRC mode. However, final decision on DRC parameters setting was also based on the validation results, namely recovery and precision. Settling time of reaction gas flow in DRC mode is approximately 30 s, therefore, we selected a single gas flow rate for all elements in a given DRC mode, which is a compromise between a total time of analysis and the efficiency of DRC to remove interferences. The selected parameters of DRC are gathered in Table 1.

### 3.2. Optimization of RPa for macroelements

The modern ICP-MS instruments are equipped with a dual stage detector that allows to measure ions in the very broad range of concentrations and still maintain a linear response of the signal intensities. This allows to measure the elements in the concentrations from less than ng L<sup>-1</sup> to hundreds of mg L<sup>-1</sup> in a single analytical run without the need to dilute the samples. However, an analysis of sample with high concentrations of elements pose the risk of saturating the detector and shortening its life span, especially for isotopes with very high abundance and low ionization potential. In biological samples, the high ion-load is often observable for bulk and macro-elements, such as Na, K, Mg, Ca and also P. The Elan software allows to measure isotopes even in high concentrations in samples after setting the specific RPa value, thus significantly reducing the ion flux for selected elements, by dynamically setting the DC voltage in the DRC rods. The RPa was optimized in standard mode for Na, K, Mg, Ca by analyzing 10 mg L<sup>-1</sup> solution of Na, K, Mg and Ca in 1% nitric acid. The results are presented in Table 3 as raw signal intensity and ratio of signals measured for given RPa to signal measured with RPa = 0. The selected parameters allowed to measure abundant elements in urine, particularly Na and K, along with the trace elements without the need to further dilute samples, and prevented the detector from overloading, which may be important in routine applications. The rejection parameters set for above elements allowed to achieve signal suppression in the orders of over 1000 fold for Na, Mg and

**Table 3**

Results of optimization of RPa parameter for 10 mg L<sup>-1</sup> of Na, Mg, K and Ca presented as raw signal intensity and ratio of signal measured with RPa = x to the signal measured with RPa = 0.

RPa value, x	Signal intensity (CPS)				Signal ratio for RPa = x/RPa = 0			
	<sup>23</sup> Na	<sup>26</sup> Mg	<sup>39</sup> K	<sup>43</sup> Ca	<sup>23</sup> Na	<sup>26</sup> Mg	<sup>39</sup> K	<sup>43</sup> Ca
0	40,857,731	4,109,892	30,868,841	111,209	–	–	–	–
0.005	37,389,379	3,923,624	33,447,941	108,661	1.1	1.0	0.9	1.0
0.01	29,928,597	3,204,828	27,739,767	86,452	1.4	1.3	1.1	1.3
0.013	16,446,558	1,621,872	13,156,676	44,124	2.5	2.5	2.3	2.5
0.015	2,628,537	365,900	1,948,922	6789	16	11	16	16
0.017	262,658	33616.5	328,654	727	156	122	94	153
0.019	35,697	3781	45,731	67	1145	1087	675	1667
0.021	5948	567	8143	47	6869	7252	3791	2381

Ca and over 600 fold for K. Similar approach was described in the application note with the procedure for natural water analysis, where trace elements were determined along with Na and K with very good recoveries [18].

### 3.3. Selection of the internal standard

The internal standard was introduced simultaneously with blanks, standards and samples in order to minimize the differences in nebulization efficiency of analyzed solutions, which might differ due to the variable matrix composition, and to overcome the potential instrumental signal drift. Four isotopes were checked as the potential ISTDs: <sup>45</sup>Sc, <sup>72</sup>Ge, <sup>103</sup>Rh and <sup>159</sup>Tb. The signal stability was checked during the validation and the analysis of urine samples. The signal of Sc showed the greatest variation between samples, thus it was rejected. The signals of Ge, Rh and Tb showed a certain variation, depending on the type of aspirated solution, and also a slight signal drift in time was observed (see Fig. 1). The selection of a specific ISTD isotope for a given analyte was based on the result of validation, namely the trueness and precision. The method of internal standard is widely used in urine analysis by ICP-MS. The ISTD solution is either aspirated by separate tubing and mixed with a sample in a T-piece, or a small volume of ISTD solution is added to all samples, standards, blanks and reference materials. The choice of ISTD elements is dependent on the analyzed elements, and in the literature the other elements selected as ISTD include: Bi, Ga, Ir, In, Y, Ho, Pt [19–24].

### 3.4. Validation of the procedure

In order to verify whether the described procedure is fit for intended purpose it was thoroughly validated. This process required multiple repetitions of blank samples, calibration standards, CRMs and spiked

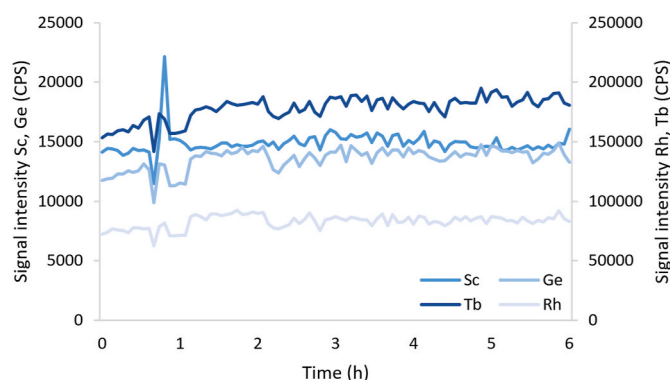


**Fig. 1.** Examination of internal standard signal stability. Intensities of internal standard isotopes – <sup>45</sup>Sc, <sup>74</sup>Ge, <sup>103</sup>Rh, <sup>159</sup>Tb – measured throughout the analysis of blanks, calibration standards, reference materials and urine samples in a single day.

samples of artificial urine. In the process of validation the important parameters characterizing the procedure were estimated: linearity of the calibration curves, limits of detection and quantification, precision and trueness. During the process of validation of the procedure, the “golden rules” of metrology, that contain general requirements for the scope and range of validation, were fulfilled, namely: (1) the entire measurement procedure, (2) the matrix variability and (3) the expected content of analyte [25].

#### 3.4.1. Linearity

The calibration curves were constructed daily and were based on the blank solution with analyte addition on 5 levels of concentration. Mean values of intensity from 3 repetitions were taken for each calibration point. The linearity of the calibration curve was assessed in two ways: as the correlation coefficient  $R$  and by the residual analysis. The calibration curve was built as the regression line using the normal least squares method. The blank sample intensity was subtracted from all intensities for standards and samples. The  $R$  coefficient provides a simple and general information on the relationship between the variables: analytical signals and concentrations of calibration standards. Usually, it is arbitrary decided that when  $R$  coefficient is greater than 0.999 or 0.9999 the relationship between measured signals and concentrations of standards are linear. The residual analysis provides more detailed information on the relation between every calibration point and the calibration curve by plotting the residuals scattered around the curve, where residuals are shown on the vertical axis and the independent variable is shown on the horizontal axis. Residual values shown on a graph should not exhibit any trends and should be randomly distributed around the horizontal axis. Examples of residual scatter plots for elements measured in standard and DRC modes are demonstrated in Fig. 2 [21,26]. Determination coefficients and analysis of residuals showed that calibration curves were linear over the whole concentration range. Linearity of the calibration curves are presented in Table 4.

#### 3.4.2. Limit of detection and limit of quantification

The suitability of the procedure to properly determine low level concentrations is called a limit of detection (LOD). It is a parameter of the analytical method that specifies the lowest level of concentration at which the analyte in the sample can be detected with specified confidence level [27]. In the analyzed sample, the concentration of analyte above LOD means that the measured signal can be reliably distinguished from the blank signal level, usually with 95% confidence level [28]. The LOD calculated in this study is also called an instrumental detection limit (IDL), and it is a parameter that reflects the detector base line noise or blank sample signal variability. LOD is estimated based on the standard deviation (SD) of the analytical signal measured for 10 separate blank solutions (1%  $\text{HNO}_3$  solution in Milli-Q water) and is calculated by

the equation:

$$LOD = \frac{3s_0}{b}$$

where  $s_0$  – SD of the blank sample signals,  $b$  – slope of the calibration curve. The limit of quantification (LOQ) is a parameter similar to the LOD but it also assumes a certain level of precision, besides the assumed confidence level [28]. LOQ is calculated in the following manner:

$$LOQ = \frac{10s_0}{b}$$

The values of LOD and LOQ are presented in Table 4. The lowest LOD was estimated for U,  $0.00023 \mu\text{g L}^{-1}$ , and highest for Ca,  $53 \mu\text{g L}^{-1}$ . The values of LOD and LOQ were estimated for all analytes in order to evaluate the scope of application of newly developed procedure. However, it must be noted that LOD and LOQ are not always important validation parameters, since macroelements (Na, Mg, K, Ca) in urine are present at much higher concentrations than LOD.

#### 3.4.3. Precision

Precision is a value that reflects the variability of the measurement data for the representative sample, with the matrix similar to the analyzed samples. In order to obtain precision, a number of repetitions (usually 10) must be performed. The value of precision is dependent on the concentration, so this parameter should be calculated for several concentration levels. In this procedure, 3 CRMs were selected with different concentrations levels and composition of matrices. The precision was further divided with regard to the time interval between the repetitions: repeatability was calculated for repeated measurement in very short time interval (during a single analytical run), and intermediate precision was calculated in broader time period (over 3 consecutive days of measurements) [29,30]. Calculations of the above mentioned parameters involved 5 independent measurements of each CRM (analyzed sequentially in a single analytical run) and 15 independent measurements of CRMs over 3 consecutive days for repeatability and intermediate precision, respectively. The parameters were evaluated using the same method, reagents and instruments, and by the same operator. Repeatability, as well as intermediate precision, were expressed in percent, as a coefficient of variation (CV), according to the formula:

$$CV = \frac{SD}{\bar{x}} \cdot 100$$

where SD – standard deviation of measured concentration,  $\bar{x}$  – mean concentration of a sample.

Obtained results for repeatability varied from 1.2% to 11% and for intermediate precision from 2% to 27%. Full information about the precision of the procedure is gathered in Table 4.

#### 3.4.4. Trueness

The trueness is a parameter that assesses the agreement between measured concentration and reference value. It is used to confirm that the applied analytical procedure provides reliable results. Trueness can be obtained by analysis of the CRM or the sample spiked with analyte. The reference value is provided in the certificate of the CRM or it is a concentration of analyte addition to the sample [30]. In this study, the trueness, expressed as a recovery in percent ( $R\%$ ), was evaluated through the analysis of three CRMs. The measurements were performed in 10 replications of 3 different CRMs and took roughly 2 h, which included potential influence of duration of instrument operation. The mean concentration value was used in order to calculate the recovery of the certified value in CRM according to the formula:

$$R\% = \frac{\bar{x}}{x_{cert}} \cdot 100$$

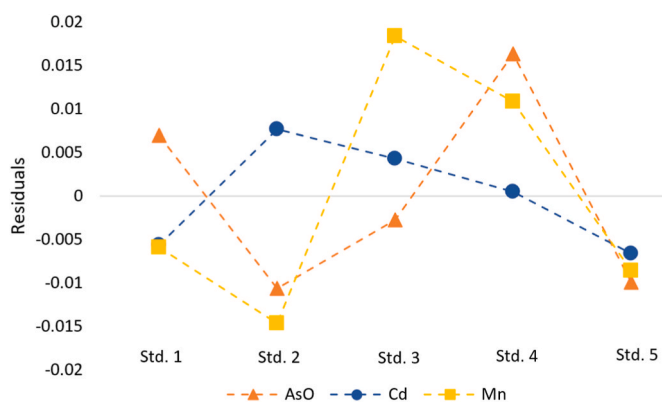


Fig. 2. Examples of residuals scatter plot based on the calibration curves of 3 analytes: As (as  $^{91}\text{AsO}$ ), Mn and Cd, measured in DRC mode with oxygen, DRC mode with ammonia and standard mode, respectively.

**Table 4**

Parameters characterizing the analytical procedure for all elements: linearity, limit of detection, limit of quantification, repeatability, intermediate precision and recovery.

Validation parameter	Li	Na	Mg	Al	K	Ca	V	Cr	Mn	Fe	Co	Cu	Zn	Se	Sr	As	Cd	Sb	Ba	Pb	U
Linearity R	0.9999	>0.9999	>0.9999	>0.9999	>0.9999	>0.9999	0.9999	0.9999	0.9999	>0.9999	>0.9999	0.9999	>0.9999	0.9998	>0.9999	>0.9999	>0.9999	>0.9999	>0.9999	0.9999	>0.9999
LOD ( $\mu\text{g L}^{-1}$ )	0.011	6.2	0.67	0.088	18	53	0.0020	0.0059	0.011	0.095	0.0022	0.011	0.057	0.20	0.0097	0.040	0.0015	0.0049	0.0033	0.0014	0.00023
LOQ ( $\mu\text{g L}^{-1}$ )	0.038	21	2.2	0.30	59	178	0.0066	0.020	0.036	0.31	0.0074	0.037	0.19	0.68	0.033	0.13	0.0048	0.016	0.011	0.0047	0.0014
Repeatability for CRMs (%)																					
SLRS-6 <sup>a</sup>	<sup>d</sup>	2.5	3.5	2.9	4.2	5.5	6.6	5.2	3.1	1.2	8.1	1.8	3.3	<sup>d</sup>	1.5	3.8	14	6.2	2.3	1.2	3.2
TM-24.4 <sup>b</sup>	2.4	<sup>d</sup>	<sup>d</sup>	1.4	<sup>d</sup>	<sup>d</sup>	2.1	2.2	2.7	1.8	3.9	1.3	<sup>d</sup>	7.8	2.6	3.5	6.0	<sup>d</sup>	1.9	2.1	2.2
Seronorm <sup>c</sup>	5.0	3.2	2.7	2.8	2.8	2.4	11	3.4	10	2.5	6.5	2.2	2.2	7.2	2.7	1.9	8.5	3.2	2.8	3.5	6.4
Intermediate precision for CRMs (%)																					
SLRS-6 <sup>a</sup>	<sup>d</sup>	18	17	13	18	20	18	19	18	4.7	18	17	25	<sup>d</sup>	12	27	11	8.7	3.1	10	2.8
TM-24.4 <sup>b</sup>	15	<sup>d</sup>	<sup>d</sup>	4.4	<sup>d</sup>	<sup>d</sup>	7.7	11	5.1	20	4.6	2.0	<sup>d</sup>	13	10	17	8.1	<sup>d</sup>	3.6	3.7	4.7
Seronorm <sup>c</sup>	4.1	6.8	5.0	22	9.2	6.5	7.6	10	16	22	10	6.9	5.2	4.2	5.9	14	14	6.6	21	12	13
Recovery for CRMs (%)																					
SLRS-6 <sup>a</sup>	<sup>d</sup>	86	91	103	88	90	103	109	108	106	116 <sup>e</sup>	85	113	<sup>d</sup>	90	105	142	107	102	113	107
TM-24.4 <sup>b</sup>	98	<sup>d</sup>	<sup>d</sup>	105	<sup>d</sup>	<sup>d</sup>	103	106	104	118	107	112	<sup>d</sup>	89	91	100	104	<sup>d</sup>	105	108	103
Seronorm <sup>c</sup>	98 <sup>e</sup>	94 <sup>e</sup>	98	119	90 <sup>e</sup>	90 <sup>e</sup>	128	92	81	92	112	85	94	130	89 <sup>e</sup>	95	136	120	86 <sup>e</sup>	110	93 <sup>e</sup>
Recovery for spiked artificial urine (%); spiked concentration:																					
0.05 $\mu\text{g L}^{-1}$	104	<LOD	<LOD	<LOD	<LOD	<LOD	109	113	119	<LOD	83	123	81	<LOD	125	88	100	93	114	78	88
1 $\mu\text{g L}^{-1}$	94	<LOD	<LOD	129	<LOD	<LOD	101	94	94	134	82	95	89	98	99	92	109	89	108	85	87
5 $\mu\text{g L}^{-1}$	84	<LOD	100	105	<LOD	<LOD	97	86	88	89	89	84	95	94	93	100	102	84	101	95	95

<sup>a</sup> SLRS-6 Riverine Water.<sup>b</sup> TM-24.4 fortified diluted lake Ontario water.<sup>c</sup> Seronorm Trace Elements Urine L-1.<sup>d</sup> Not certified.<sup>e</sup> Reference value.

**Table 5**  
Values of main uncertainty sources and the resulting expanded uncertainty, with coverage factor  $k = 2$ , obtained for analyzed elements.

uncertainty parameter	Li	Na	Mg	Al	K	Ca	V	Cr	Mn	Fe	Co	Cu	Zn	Se	Sr	As	Cd	Sb	Ba	Pb	U
$u_R$	0.043	0.067	0.100	0.316	0.083	0.059	0.138	0.101	0.100	0.131	0.123	0.089	0.097	0.134	0.052	0.109	0.298	0.187	0.176	0.282	0.125
$u_{cal}$	0.067	0.070	0.049	0.039	0.068	0.038	0.133	0.110	0.171	0.068	0.074	0.055	0.064	0.200	0.038	0.118	0.089	0.194	0.059	0.059	0.053
$u_{prec}$	0.051	0.012	0.013	0.110	0.012	0.017	0.086	0.054	0.070	0.020	0.090	0.015	0.017	0.061	0.015	0.121	0.116	0.040	0.018	0.047	0.070
$u_c$	0.094	0.097	0.112	0.337	0.108	0.072	0.210	0.159	0.210	0.149	0.169	0.106	0.118	0.249	0.066	0.201	0.332	0.273	0.187	0.292	0.153
U	0.189	0.195	0.224	0.674	0.216	0.143	0.420	0.317	0.420	0.298	0.339	0.211	0.235	0.497	0.132	0.402	0.664	0.546	0.373	0.585	0.305
U (%)	18.9	19.5	22.4	67.4	21.6	14.3	42.0	31.7	42.0	29.8	33.9	21.1	23.5	49.7	13.2	40.2	66.4	54.6	37.3	58.5	30.5

$u_R$  – uncertainty component associated with recovery.  
 $u_{cal}$  – uncertainty component associated with calibration.  
 $u_{prec}$  – uncertainty component associated with precision.  
 $u_c$  – combined standard uncertainty.  
 U - expanded uncertainty.

**Table 6**  
Statistical description of the 21 elements determination results in fetal urine samples (n = 58). The values lower than LOD are included in mean, median and interquartile range.

Concentration of elements in urine samples ( $\mu\text{g L}^{-1}$ )	Li	Na	Mg	Al	K	Ca	V	Cr	Mn	Fe	Co	Cu	Zn	Se	Sr	As	Cd	Sb	Ba	Pb	U
Mean	1.2	1,687,071	13,375	11	209,298	45,419	0.19	0.54	0.45	27	0.12	23	270	11	20	1.0	0.058	0.33	1.9	0.19	0.0035
Median	0.84	1,850,395	12,116	8.1	143,979	42,412	0.20	0.28	0.40	18	0.10	17	47	8.1	18	0.76	0.033	0.37	0.65	0.13	0.0032
Interquartile range	0.88	1,248,087	7203	7.3	142,388	43,391	0.11	0.29	0.28	15	0.084	16	123	4.0	12	0.77	0.036	0.31	0.99	0.20	0.0011
Minimum value	<LOD	44,722	1018	3.9	52,782	3388	0.020	<LOD	<LOD	2.5	<LOD	2.2	7.8	3.2	2.9	<LOD	<LOD	<LOD	0.20	<LOD	<LOD
Maximum value	8.7	2,974,054	38,011	44	651,107	105,734	0.35	7.7	1.4	228	0.44	130	9706	181	53	3.1	0.57	0.74	27	0.64	0.0093
5th percentile of values range	0.22	260,294	2659	4.8	65,832	7408	0.075	0.071	0.16	5.1	0.041	6.7	13	3.8	6.4	0.41	0.016	0.072	0.32	0.037	0.0024
95th percentile of values range	3.3	2,759,280	28,699	23	597,182	87,522	0.30	0.98	0.87	82	0.23	76	481	15	44	2.6	0.089	0.60	5.7	0.48	0.0054

LOD – limit of detection (See Table 4).

where  $x_{\text{cert}}$  – reference value taken from the certificate of the CRM. Obtained results for all elements, which vary from 75% to 125%, are acceptable, meeting the criterion recommended by the US EPA method 6020B for elemental analysis by ICP-MS [31].

The Student's t-test was performed to verify if obtained mean recoveries were significantly different from 100%. The t value was calculated according to the equation:

$$t = \frac{|R_x - 1|}{u(R_x)}$$

where  $R_x$  – mean recovery and  $u(R_x)$  – standard uncertainty of analyte recovery. The Student's t-test confirmed that calculated recoveries were in good agreement with certified values for all determined elements. The additional assessment of trueness was performed by analyzing spiked artificial urine on the levels of concentrations:  $0.05 \mu\text{g L}^{-1}$ ,  $1 \mu\text{g L}^{-1}$  and  $5 \mu\text{g L}^{-1}$ . The recoveries of the certified concentrations of determined elements and of the spiked artificial urine are presented in Table 4.

### 3.5. Properties of the measurement result

#### 3.5.1. Traceability statement

The traceability of the measurement result in this study was established by analysis of the CRMs with stated uncertainties, and also by the standard addition method to the artificial matrix, similar to the real sample matrix, using the standard solutions of elements with stated uncertainties [32]. The matrix matched CRM used in the study was Seronorm Trace Elements Urine L1.

#### 3.5.2. Measurement uncertainty

The final measurement result is affected by all steps of the analytical procedure, which includes among others: the sample preparation, calibration, optimization and the final measurement. Each analytical step may have more or less significant impact on the final result, and it is important to assess and include those factors in the form of uncertainty of the measurement result. The uncertainty budget was calculated by using the mathematical description and propagation of error approach with the input value based on the repeated measurement of the real urine sample, the CRM sample, and also by including the data provided in certificates by the manufacturers of the measuring glassware and standards. All major uncertainty source was included in the uncertainty budget and finally expressed as the expanded uncertainty with 95% confidence level [33].

In this study, the measurement uncertainty was estimated based on 3 major uncertainty components associated with: (a) calibration, (b) precision of the sample measurement and (c) recovery of the reference value of CRM. The component associated with the calibration included the data provided in the certificates by the manufacturers of the multi-element standard solution, the automatic pipettes and the measuring flasks, and also the precision of measured signals of each calibration standard; it is calculated with the equation:

$$u_{\text{cal}} = \sqrt{\left(\frac{u(c_{\text{std}})}{c_{\text{std}}}\right)^2 + \sum_{i=1}^m \left(\frac{u(V_p)}{V_p}\right)^2 + \sum_{i=1}^m \left(\frac{u(V_k)}{V_k}\right)^2 + \sum_{i=1}^m \left(\frac{RSD_m}{\sqrt{n_m}}\right)^2}$$

where  $u_{\text{cal}}$  – uncertainty component associated with calibration;  $u(c_{\text{std}})$  – standard uncertainty of the standard solution concentration;  $c_{\text{std}}$  – concentration of the standard solution;  $m$  – number of calibration solutions;  $u(V_p)$  – standard uncertainty of the automatic pipette volume;  $V_p$  – automatic pipette volume;  $u(V_k)$  – standard uncertainty of the measuring flask volume;  $V_k$  – measuring flask volume;  $RSD_m$  – relative standard deviation of the m-th calibration solution;  $n_m$  – number of repetitions of m-th calibration solution ( $n_m = 3$ ). The dispersion of the measured concentration for the real urine sample was incorporated in the component associated with the precision, calculated with the formula:

$$u_{\text{prec}} = \frac{RSD_x}{\sqrt{n_s}}$$

where  $u_{\text{prec}}$  – uncertainty component associated with precision;  $RSD_x$  – relative standard deviation of the single urine sample;  $n_s$  – number of repetitions of the single urine sample ( $n_s = 3$ ). For this calculation, a urine sample, for which measured concentrations of all analytes were  $> \text{LOD}$ , was taken. The component associated with recovery is taking into consideration the concentration and standard deviation of measured CRM sample, the certified values of concentration and uncertainty provided by the manufacturer of the CRM, and the recovery value obtained in the validation; it is calculated with the formula:

$$u_R = R_x \cdot \sqrt{\left(\frac{s_{\text{obs}}}{n_{\text{obs}} \cdot c_{\text{obs}}}\right)^2 + \left(\frac{u(c_{\text{CRM}})}{c_{\text{CRM}}}\right)^2}$$

where  $u_R$  – uncertainty component associated with recovery;  $s_{\text{obs}}$  – standard deviation of measured CRM;  $n_{\text{obs}}$  – number of repetitions of measured CRM ( $n_{\text{obs}} = 5$ );  $c_{\text{obs}}$  – mean concentration of measured CRM;  $u(c_{\text{CRM}})$  – standard uncertainty of the reference value of CRM;  $c_{\text{CRM}}$  – reference value of CRM. In order to avoid significant underestimation of uncertainty for elements with no stated uncertainty of reference value in the certificate of CRM, which regards elements with informative value, the parameter  $u(c_{\text{CRM}})$  was replaced with  $s_{\text{obs}}$ ; in the case of Seronorm Trace Elements Urine L-1, this concerns elements: Li, Na, K, Ca, Se, Ba and U. The calculated main 3 uncertainty components are then combined into the combined standard uncertainty, using the formula:

$$u_c = \sqrt{(u_{\text{cal}})^2 + (u_{\text{prec}})^2 + (u_R)^2}$$

where  $u_c$  – combined standard uncertainty. The expanded uncertainty was calculated by multiplication of the combined standard uncertainty and the coverage factor  $k = 2$ , which corresponds to the confidence level 95%.

$$U = u_c \cdot k$$

where  $U$  – expanded uncertainty;  $k$  – coverage factor.

The expanded uncertainty  $U$  is a relative value, and in order to obtain the absolute uncertainty it is multiplied by the concentration measured for a urine sample. The obtained values of expanded uncertainty, combined standard uncertainty, as well as three main uncertainty components – associated with calibration, precision and recovery – are presented in Table 5. The lowest expanded uncertainties, with the values 13.2% and 14.3%, were estimated for Sr and Ca, respectively. The highest expanded uncertainties, with values 67.4% and 66.4%, were estimated for Al and Cd, respectively. Such high values of uncertainties are expected for elements occurring in ultra-trace levels and in rich matrices, so it is very common to obtain high precision values. Also, large uncertainties of the certified concentrations in certificate of CRM may have significant influence on the uncertainty budget.

### 3.6. Application of the procedure for fetal urine analysis

The developed and validated analytical procedure for the determination of 21 macro- and trace elements in small volumes of fetal urine was applied to the 58 real samples collected from human fetuses. The results of the analysis are presented in Table 6 as the mean and median values, and also by the parameters of basic descriptive statistics. The values below LOD for a given element were included in the mean, median and interquartile range (IQR) in order to allow the statistical calculations and to avoid data bias caused by the arbitrary change or rejection of values below LOD. However, it must be noted that measurements below LOD have very large uncertainties, which is expected for the concentrations close to the blank level. The distribution of data is not normal, therefore, IQR is used to describe the 25%–75% range of all

values. For several elements, like Zn, Se and Cr the min-max range is much higher than the IQR, which is due to the large spikes of concentrations in few analyzed samples.

The elements As, Cd and Cr were detected in 47%–66% of the samples, and Sb and U were detected only in less than 31% of samples. The concentrations of the rest of the elements were determined as >LOD in more than 95% of the urine samples. Comparison of the mean concentrations with the values measured in the non-occupationally exposed healthy adult population shows that concentration of toxic elements, As, Cd and Pb is significantly lower in fetal urine, and the concentrations of physiological elements, V, Cr, Mn and Cu is higher or similar [9]. Different study performed in Canada on healthy non-exposed volunteers provides the similar conclusion for median concentrations of toxic elements, however, the physiological elements in our study were on similar levels or lower [34]. The comparison with literature data suggests that concentrations of toxic elements is lower in the urine of fetus in comparison with the urine of adult, which might be due to the additional mechanisms of protection from xenobiotics in the mother's placenta [35].

#### 4. Conclusions

The ICP-MS is an outstanding technique for multielemental analysis of practically every sample, including the body fluids. It is often of vital importance to provide complex information for samples, like urine, serum or blood for various reasons, including medical diagnostics, forensics, population research and more. The ICP-MS provides excellent limits of detection and precision and the latest generations of instruments allow to efficiently minimize the influence of interferences, which can dramatically improve detection capability. Simultaneously, the improvements in sample introduction techniques allow to obtain reliable results with lower sample volumes. In this study, the application of micronebulizer, as well as the ammonia and oxygen gases in the dynamic reaction cell in ICP-MS apparatus, allowed to determine concentrations of 21 macro- and trace elements, Li, Na, Mg, Al, K, Ca, V, Cr, Mn, Fe, Co, Cu, Zn, Se, Sr, As, Cd, Sb, Ba, Pb and U, with broad concentrations range, in urine collected from human fetuses. A new procedure was developed, which allowed to analyze scarce amounts of sample with volume of 200  $\mu\text{L}$  without the need of time-consuming sample digestion in closed microwave systems. The procedure and ICP-MS instrument were thoroughly optimized, including the complete optimization of DRC parameters: gas flow, RPq and RPa. The use of RPa for macroelements – Na, K, Ca and Mg – allowed to determine the concentrations of up to 300  $\text{mg L}^{-1}$ , alongside with the trace elements in the single analytical run. The metrological rules were applied: (1) the procedure was validated by estimating the characteristic parameters of the procedure, (2) the traceability of the measurement result was established and (3) the uncertainty of the measurement result was estimated, based on the parameters associated with calibration, precision and recovery. The limits of detection were in the range: (0.00023–53  $\mu\text{g L}^{-1}$ ) for U and Ca, respectively. The recoveries of the reference value of Seronorm Trace Elements Urine L-1 were in the range: 81%–136% for Mn and Cd, respectively. The traceability of the measurement result was established by the analysis of matrix-matched CRM – Seronorm Trace Elements Urine L-1 – and by the analyte addition method to the artificial matrix. The expanded relative uncertainties ( $k = 2$ ) were estimated in the range: 13%–66% for Sr and Cd, respectively. The developed and validated procedure was applied for the analysis of 58 urine samples collected from human fetuses. The comparison of results with the literature suggests that the concentration of toxic elements, As, Cd and Pb, is lower in fetal urine than in the adult urine. However, the comparison of measured concentrations of physiological elements with the literature provides no definitive conclusions.

#### Credit author statement

Adam Sajnog: Conceptualization, Methodology, Validation, Formal analysis, Investigation, Writing, Visualization, Project administration; Danuta Baraikiewicz: Conceptualization, Methodology, Writing, Supervision, Project administration, Funding acquisition; Marcin Tkaczyk: Investigation, Supervision, Funding acquisition; Małgorzata Stańczyk: Investigation; Krzysztof Szaflik: Investigation; Joanna Suliburska: Conceptualization, Investigation, Resources; Rafał Kocylowski: Conceptualization, Investigation, Resources.

#### Declaration of competing interest

The authors declare that they have no known competing financial interests or personal relationships that could have appeared to influence the work reported in this paper.

#### Acknowledgement

The study was granted by Polish Mothers Memorial Hospital Research Institute – internal grant 2016/IV/54-GW. This research was financially supported by the Ministry of Science and Higher Education in Poland for statutory activities in Adam Mickiewicz University, Poznań.

#### Appendix A. Supplementary data

Supplementary data to this article can be found online at <https://doi.org/10.1016/j.talanta.2020.121672>.

#### References

- [1] M.N. Bor, F. Usul, M. Ergin, Circulation of amniotic fluid contents. Pathway of  $^{22}\text{Na}$  from amniotic fluid to fetal and maternal organs, *Arch. Int. Physiol. Biochim.* 76 (1968) 833–840.
- [2] M. Fägerquist, U. Fägerquist, A. Odén, S.G. Blomberg, Fetal urine production and accuracy when estimating fetal urinary bladder volume, *Ultrasound Obstet. Gynecol.* 17 (2001) 132–139, <https://doi.org/10.1046/j.1469-0705.2001.00294.x>.
- [3] F. Manoni, G. Gessoni, M.G. Alessio, A. Caleffi, G. Sacconi, M.G. Silvestri, D. Poz, M. Ercolin, A. Tinello, S. Valverde, C. Ottomano, G. Lippi, Mid-stream vs. first-voided urine collection by using automated analyzers for particle examination in healthy subjects: an Italian multicenter study, *Clin. Chem. Lab. Med.* 50 (2012) 679–684, <https://doi.org/10.1515/cclm.2011.823>.
- [4] N.A. Brunzel, *Fundamentals of Urine and Body Fluid Analysis, fourth ed.*, Elsevier, St. Louis, Missouri, 2018.
- [5] I.M.M. Kenawy, M.A.H. Hafez, M.A. Akl, R.R. Lashein, Determination by AAS of some trace heavy metal ions in some natural and biological samples after their preconcentration using newly chemically modified chloromethylated polystyrene-PAN ion-exchanger, *Anal. Sci.* 16 (2000) 493–500, <https://doi.org/10.2116/analsci.16.493>.
- [6] T. Guo, J. Baasner, Determination of mercury in urine by flow-injection cold vapour atomic absorption spectrometry, *Anal. Chim. Acta* 278 (1993) 189–196, [https://doi.org/10.1016/0003-2670\(93\)80096-4](https://doi.org/10.1016/0003-2670(93)80096-4).
- [7] T.-W. Lin, S.-D. Huang, Direct and simultaneous determination of copper, chromium, aluminum, and manganese in urine with a multielement graphite furnace atomic absorption spectrometer, *Anal. Chem.* 73 (2001) 4319–4325, <https://doi.org/10.1021/ac010319h>.
- [8] J.S. Suleiman, B. Hu, C. Huang, N. Zhang, Determination of Cd, Co, Ni and Pb in biological samples by microcolumn packed with black stone (Pierre noire) online coupled with ICP-OES, *J. Hazard Mater.* 157 (2008) 410–417, <https://doi.org/10.1016/j.jhazmat.2008.01.014>.
- [9] P. Heitland, H.D. Köster, Fast, simple and reliable routine determination of 23 elements in urine by ICP-MS, *J. Anal. At. Spectrom.* 19 (2004) 1552–1558, <https://doi.org/10.1039/B410630J>.
- [10] M.H. Nguyen, T.D. Pham, T.L. Nguyen, H.A. Vu, T.T. Ta, M.B. Tu, T.H.Y. Nguyen, D.B. Chu, Speciation analysis of arsenic compounds by HPLC-ICP-MS: application for human serum and urine, *J. Anal. Methods Chem.* 2018 (2018) 1–8, <https://doi.org/10.1155/2018/9462019>.
- [11] X. Yu, C. Liu, Y. Guo, T. Deng, Speciation analysis of trace arsenic, mercury, selenium and antimony in environmental and biological samples based on hyphenated techniques, *Molecules* 24 (2019) 926, <https://doi.org/10.3390/molecules24050926>.
- [12] M. Aramendía, L. Rello, F. Vanhaecke, M. Resano, Direct trace-elemental analysis of urine samples by laser ablation-inductively coupled plasma mass spectrometry after sample deposition on clinical filter papers, *Anal. Chem.* 84 (2012) 8682–8690, <https://doi.org/10.1021/ac3018839>.
- [13] U. Kumtaptim, A. Siripinyanond, C. Auray-Blais, A. Ntwari, J.S. Becker, Analysis of trace metals in single droplet of urine by laser ablation inductively coupled plasma

- mass spectrometry, *Int. J. Mass Spectrom.* 307 (2011) 174–181, <https://doi.org/10.1016/j.ijms.2011.01.030>.
- [14] R.F.J. Dams, J. Goossens, L. Moens, Spectral and non-spectral interferences in inductively coupled plasma mass-spectrometry, *Mikrochim. Acta* 119 (1995) 277–286, <https://doi.org/10.1007/BF01244007>.
- [15] T.W. May, R.H. Wiedmeyer, M. Chaudhary-webb, D.C. Paschal, W.C. Elliott, H. P. Hopkins, a M. Ghazi, B.C. Ting, I. Romieu, O. Vicente, E. Pelfort, L. Martinez, R. Olsina, E. Marchevsky, H.P. Chen, D.T. Miller, J.C. Morrow, A table of polyatomic interferences in ICP-MS, *At. Spectrosc.* 19 (1998) 150–155.
- [16] S.D. Tanner, V.I. Baranov, U. Vollkopf, A dynamic reaction cell for inductively coupled plasma mass spectrometry (ICP-DRC-MS), *J. Anal. At. Spectrom.* 15 (2000) 1261–1269, <https://doi.org/10.1039/b002604m>.
- [17] PerkinElmer Inc, *Sensitivity, Background, Noise, and Calibration in Atomic Spectroscopy: Effects on Accuracy and Detection Limits*, 2018.
- [18] K. Neubauer, *The Analysis of Soils and Waters in Accordance with U.S. EPA Method 6020B Using the NexION 2000 ICP-MS*, 2017. [http://www.perkinelmer.ca/lab-solutions/resources/docs/APP-NexION-2000-ICP-MS-Soils-Waters-EPA-602-0-013259\\_01.pdf](http://www.perkinelmer.ca/lab-solutions/resources/docs/APP-NexION-2000-ICP-MS-Soils-Waters-EPA-602-0-013259_01.pdf). (Accessed 16 June 2020).
- [19] G. Paglia, O. Miedico, M. Tarallo, A.R. Lovino, G. Astarita, A.E. Chiaravalle, G. Corso, Evaluation of seasonal variability of toxic and essential elements in urine analyzed by inductively coupled plasma mass spectrometry, *Expo. Heal.* 9 (2017) 79–88, <https://doi.org/10.1007/s12403-016-0222-x>.
- [20] K.-Y. Choe, R. Gajek, Determination of trace elements in human urine by ICP-MS using sodium chloride as a matrix-matching component in calibration, *Anal. Methods*. 8 (2016) 6754–6763, <https://doi.org/10.1039/C6AY01877G>.
- [21] F. Ruggieri, A. Alimonti, B. Bocca, Full validation and accreditation of a method to support human biomonitoring studies for trace and ultra-trace elements, *TrAC Trends Anal. Chem.* 80 (2016) 471–485, <https://doi.org/10.1016/j.trac.2016.03.023>.
- [22] B.M. Freire, T. Pedron, C.N. Lange, L.R. Sanches, G.R.M. Barcelos, W.R.P. Filho, B. L. Batista, Calibration for the determination of 19 trace elements in serum and urine, *Toxicol. Environ. Chem.* 100 (2018) 395–412, <https://doi.org/10.1080/02772248.2018.1537397>.
- [23] J. Morton, E. Tan, E. Leese, J. Cocker, Determination of 61 elements in urine samples collected from a non-occupationally exposed UK adult population, *Toxicol. Lett.* 231 (2014) 179–193, <https://doi.org/10.1016/j.toxlet.2014.08.019>.
- [24] M.G. Minnich, D.C. Miller, P.J. Parsons, Determination of As, Cd, Pb, and Hg in urine using inductively coupled plasma mass spectrometry with the direct injection high efficiency nebulizer, *Spectrochim. Acta Part B At. Spectrosc.* 63 (2008) 389–395, <https://doi.org/10.1016/j.sab.2007.11.033>.
- [25] E. Bulska, *Lecture Notes in Chemistry 101 Metrology in Chemistry*, Springer Nature Switzerland AG, Cham, Switzerland, 2018. <http://www.springer.com/series/632>.
- [26] F. Raposo, Evaluation of analytical calibration based on least-squares linear regression for instrumental techniques: a tutorial review, *TrAC Trends Anal. Chem.* 77 (2016) 167–185, <https://doi.org/10.1016/j.trac.2015.12.006>.
- [27] M. Belter, A. Sajnóg, D. Baratkiewicz, Over a century of detection and quantification capabilities in analytical chemistry - historical overview and trends, *Talanta* 129 (2014) 606–616, <https://doi.org/10.1016/j.talanta.2014.05.018>.
- [28] L.A. Currie, Nomenclature in evaluation of analytical methods including detection and quantification capabilities (IUPAC Recommendations 1995), *Pure Appl. Chem.* 67 (1995) 1699–1723, [https://doi.org/10.1016/S0003-2670\(99\)00104-X](https://doi.org/10.1016/S0003-2670(99)00104-X).
- [29] Joint Committee For Guides In Metrology, *Vocabulaire international de métrologie*, *VIM3 Int. Vocab. Metrol.* 3 (2012) 104, [https://doi.org/10.1016/0263-2241\(85\)90006-5](https://doi.org/10.1016/0263-2241(85)90006-5).
- [30] B. Magnusson, U. Örnemark (Eds.), *Eurachem Guide: the Fitness for Purpose of Analytical Methods – A Laboratory Guide to Method Validation and Related Topics*, second ed., Eurachem, 2014.
- [31] U.S. EPA, *Method 6020B (SW-846): inductively coupled plasma-mass spectrometry, Revision 2 (2014)*.
- [32] P. Quevauviller, Traceability of environmental chemical measurements, *TrAC Trends Anal. Chem.* 23 (2004) 171–177, [https://doi.org/10.1016/S0165-9936\(04\)00314-0](https://doi.org/10.1016/S0165-9936(04)00314-0).
- [33] V.J. Barwick, S.L.R. Ellison, Measurement uncertainty: approaches to the evaluation of uncertainties associated with recovery†, *Analyst* 124 (1999) 981–990, <https://doi.org/10.1039/a901845j>.
- [34] J.-P. Goullé, L. Mahieu, J. Castermant, N. Neveu, L. Bonneau, G. Lainé, D. Bouige, C. Lacroix, Metal and metalloid multi-elementary ICP-MS validation in whole blood, plasma, urine and hair, *Forensic Sci. Int.* 153 (2005) 39–44, <https://doi.org/10.1016/j.forsciint.2005.04.020>.
- [35] C. Gundacker, M. Hengstschläger, The role of the placenta in fetal exposure to heavy metals, *Wien Med. Wochenschr.* 162 (2012) 201–206, <https://doi.org/10.1007/s10354-012-0074-3>.

## Supplementary material

A new procedure for determination of macro- and trace elements in human fetus urine by ICP-DRC-MS equipped with a micro-flow nebulizer. Validation and uncertainty estimation

Adam Sajnog<sup>1,2</sup>, Marcin Tkaczyk<sup>3</sup>, Małgorzata Stańczyk<sup>3</sup>, Krzysztof Szaflik<sup>4</sup>, Joanna Suliburska<sup>5</sup>, Rafał Kocylowski<sup>6</sup>, Danuta Barańkiewicz<sup>1</sup>

- 1) Department of Trace Analysis, Faculty of Chemistry, Adam Mickiewicz University, Poznań, ul. Uniwersytetu Poznańskiego 8, 61–614 Poznań, Poland
- 2) Center for Advanced Technology, Adam Mickiewicz University, Poznań, ul. Uniwersytetu Poznańskiego 10, 61–614 Poznań, Poland
- 3) Department of Pediatrics, Immunology and Nephrology, Polish Mother's Memorial Hospital Research Institute, ul. Rzgowska 281/289, 93–338 Łódź, Poland
- 4) Department of Gynecology, Fertility and Fetal Therapy, Polish Mother's Memorial Hospital Research Institute, ul. Rzgowska 281/289, 93–338 Łódź, Poland
- 5) Institute of Human Nutrition and Dietetics, Poznan University of Life Sciences, ul. Wojska Polskiego 31, 60–624 Poznań, Poland; e-mail: joanna.suliburska@up.poznan.pl
- 6) PreMediCare New Med Medical Center, ul. Drużbickiego 13, 61–693 Poznań, Poland, e-mail: info@premedicare.pl

Corresponding Author: Adam Sajnog

E-mail address: [adam.sajnog@amu.edu.pl](mailto:adam.sajnog@amu.edu.pl)

Tel. +48 61 829 1606, fax +48 61 829 1555

Table S.1 Natural abundance and examples of spectral interferences for selected isotopes

Isotope (natural abundance)	Polyatomic spectral interferences
$^{27}\text{Al}$ (100%)	$^{12}\text{C}^{15}\text{N}^+$ , $^{12}\text{C}^{14}\text{N}^1\text{H}^+$ , $^{13}\text{C}^{14}\text{N}^+$
$^{51}\text{V}$ (99.8%)	$^{35}\text{Cl}^{16}\text{O}^+$ , $^{36}\text{Ar}^{15}\text{N}^+$ , $^{38}\text{Ar}^{13}\text{C}^+$ , $^{36}\text{Ar}^{14}\text{N}^1\text{H}^+$ , $^{34}\text{S}^{16}\text{O}^1\text{H}^+$ , $^{37}\text{Cl}^{14}\text{N}^+$
$^{52}\text{Cr}$ (83.8%)	$^{40}\text{Ar}^{12}\text{C}^+$ , $^{36}\text{Ar}^{16}\text{O}^+$ , $^{38}\text{Ar}^{14}\text{N}^+$ , $^{35}\text{Cl}^{16}\text{O}^1\text{H}^+$ , $^{37}\text{Cl}^{15}\text{N}^+$
$^{55}\text{Mn}$ (100%)	$^{40}\text{Ar}^{14}\text{N}^1\text{H}^+$ , $^{40}\text{Ar}^{15}\text{N}^+$ , $^{38}\text{Ar}^{16}\text{O}^1\text{H}^+$ , $^{39}\text{K}^{16}\text{O}^+$ ,
$^{56}\text{Fe}$ (91.7%)	$^{40}\text{Ar}^{16}\text{O}^+$ , $^{40}\text{Ar}^{15}\text{N}^1\text{H}^+$ , $^{40}\text{Ca}^{16}\text{O}^+$ , $^{37}\text{Cl}^{18}\text{O}^1\text{H}^+$
$^{63}\text{Cu}$ (69.2%)	$^{40}\text{Ar}^{23}\text{Na}^+$ , $^{23}\text{Na}^{40}\text{Ca}^+$ , $^{16}\text{O}^{12}\text{C}^{35}\text{Cl}^+$ , $^{14}\text{N}^{12}\text{C}^{37}\text{Cl}^+$ , $^{31}\text{P}^{16}\text{O}_2^+$
$^{64}\text{Zn}$ (48.6%)	$^{32}\text{S}^{16}\text{O}_2^+$ , $^{31}\text{P}^{16}\text{O}_2^1\text{H}^+$ , $^{48}\text{Ca}^{16}\text{O}^+$ , $^{32}\text{S}^{2+}$ , $^{36}\text{Ar}^{14}\text{N}^{2+}$
$^{75}\text{As}$ (100%)	$^{40}\text{Ar}^{35}\text{Cl}^+$ , $^{36}\text{Ar}^{38}\text{Ar}^1\text{H}^+$ , $^{36}\text{Ar}^{39}\text{K}^+$ , $^{43}\text{Ca}^{16}\text{O}_2^+$ , $^{23}\text{Na}^{12}\text{C}^{40}\text{Ar}^+$
$^{82}\text{Se}$ (8.82%)	$^{40}\text{Ar}^{42}\text{Ca}^+$ , $^{40}\text{Ar}_2^1\text{H}_2^+$ , $^{34}\text{S}^{16}\text{O}_3^+$ , $^{12}\text{C}^{35}\text{Cl}_2^+$ ,

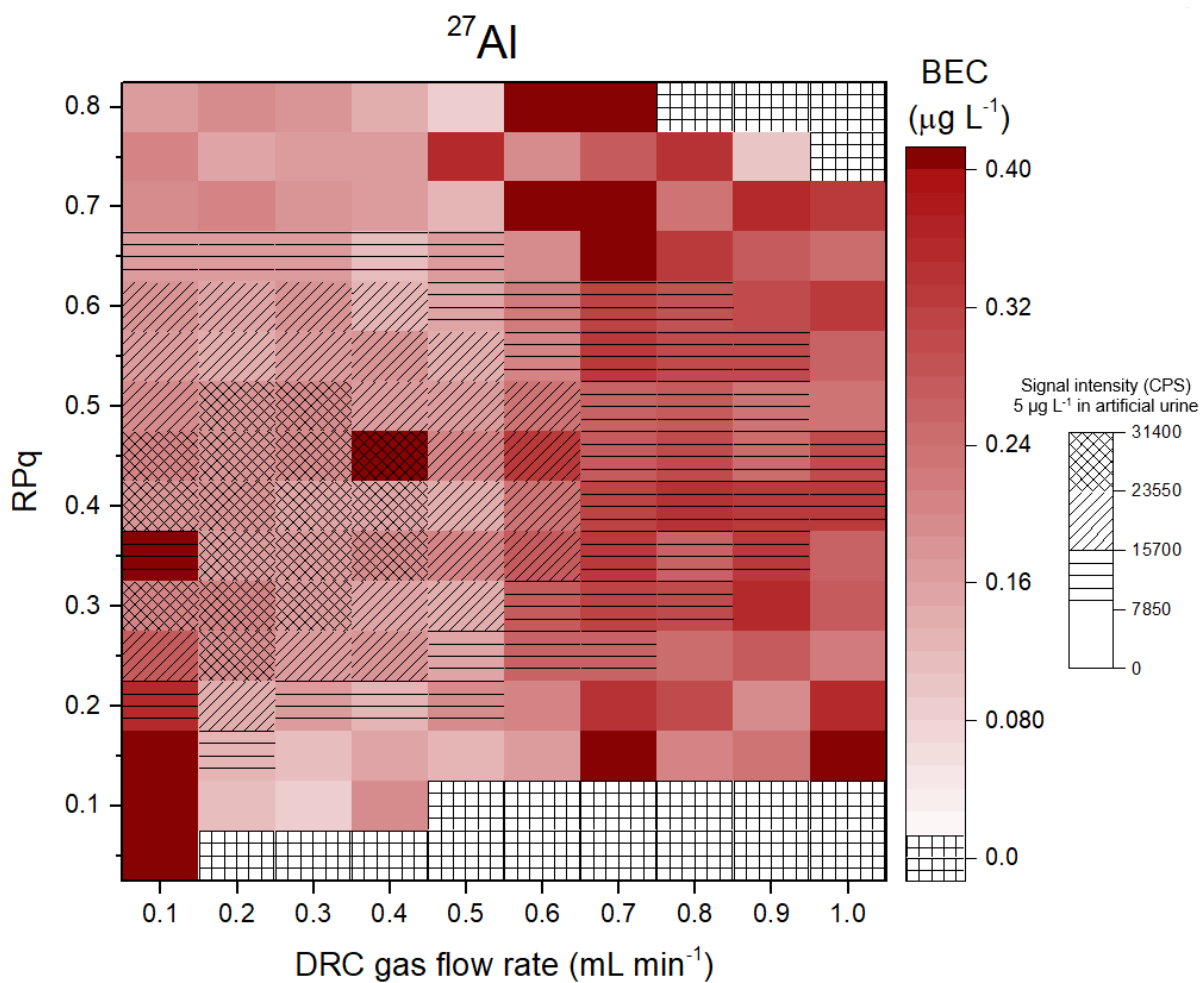


Fig. S.1 Results of DRC optimization (ammonia flow rate and RPq) in artificial urine spiked with 5  $\mu\text{g L}^{-1}$  of aluminium. BEC represents a background equivalent concentrations of blank sample (unspiked artificial urine). Signal intensity (in CPS) measured for artificial urine spiked with 5  $\mu\text{g L}^{-1}$  of Al is represented as textured rectangles in graph.

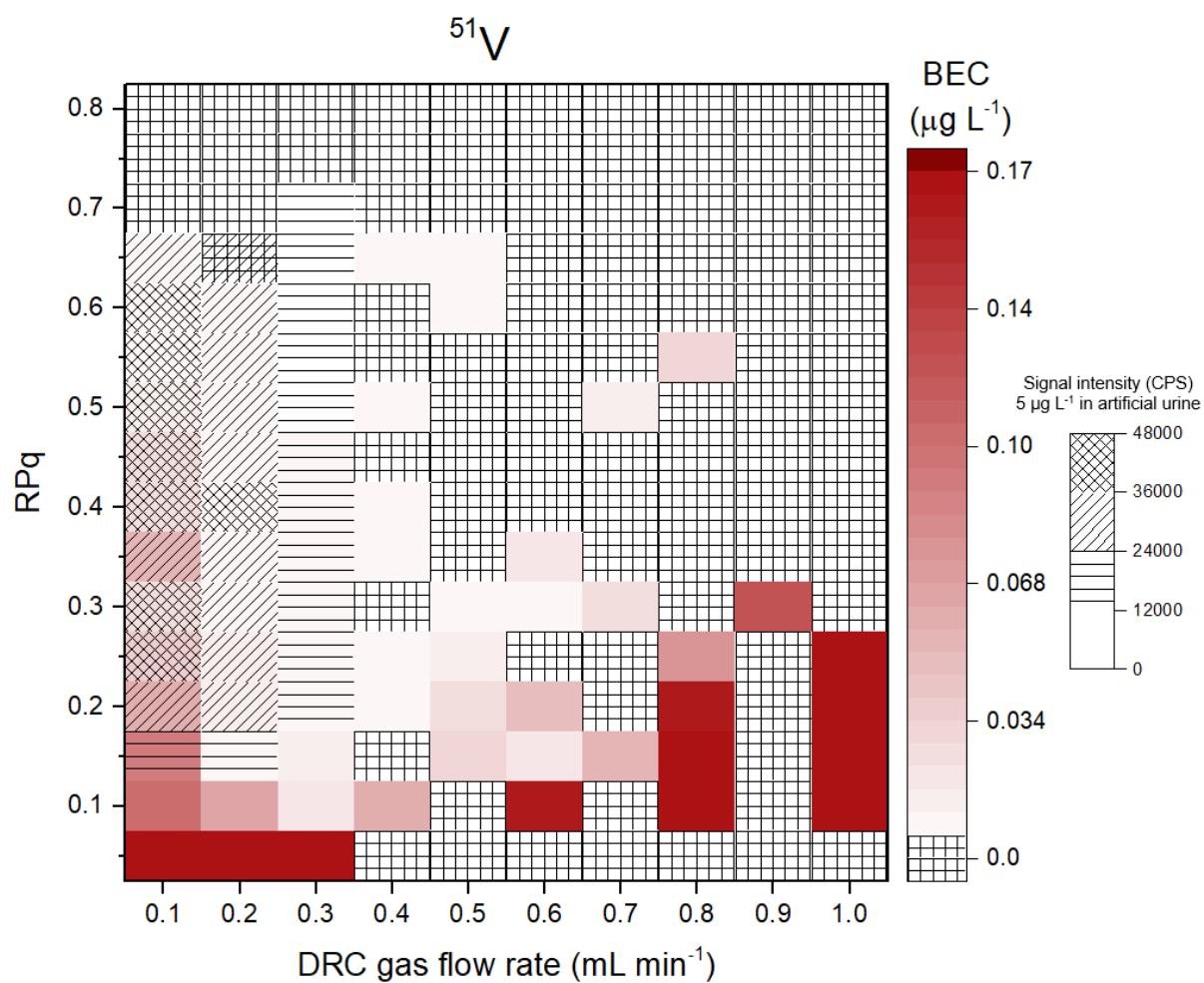


Fig. S.2 Results of DRC optimization (ammonia flow rate and RPq) in artificial urine spiked with 5  $\mu\text{g L}^{-1}$  of vanadium. BEC represents a background equivalent concentrations of blank sample (unspiked artificial urine). Signal intensity (in CPS) measured for artificial urine spiked with 5  $\mu\text{g L}^{-1}$  of V is represented as textured rectangles in graph.

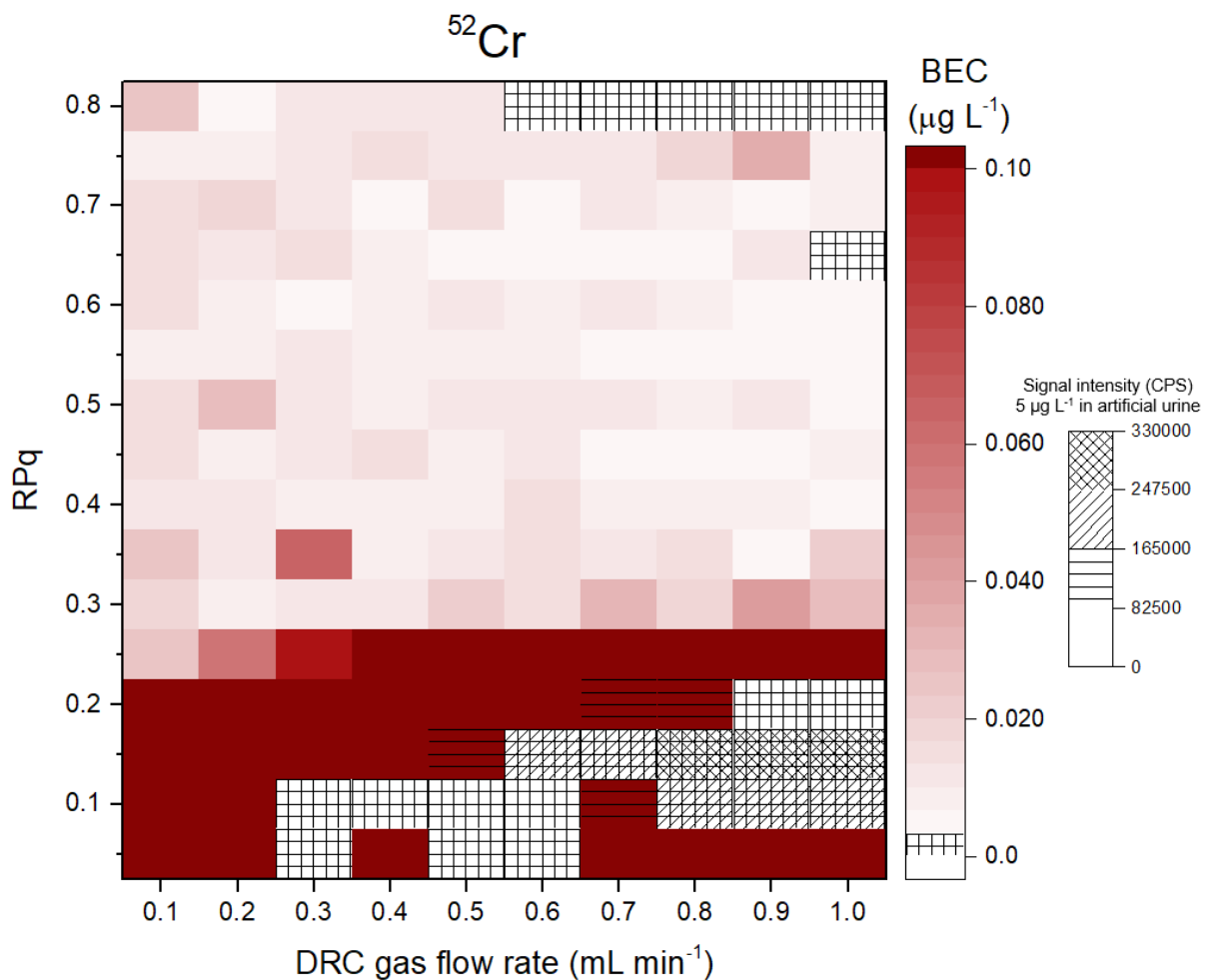


Fig. S.3 Results of DRC optimization (ammonia flow rate and RPq) in artificial urine spiked with 5  $\mu\text{g L}^{-1}$  of chromium. BEC represents a background equivalent concentrations of blank sample (unspiked artificial urine). Signal intensity (in CPS) measured for artificial urine spiked with 5  $\mu\text{g L}^{-1}$  of Cr is represented as textured rectangles in graph.

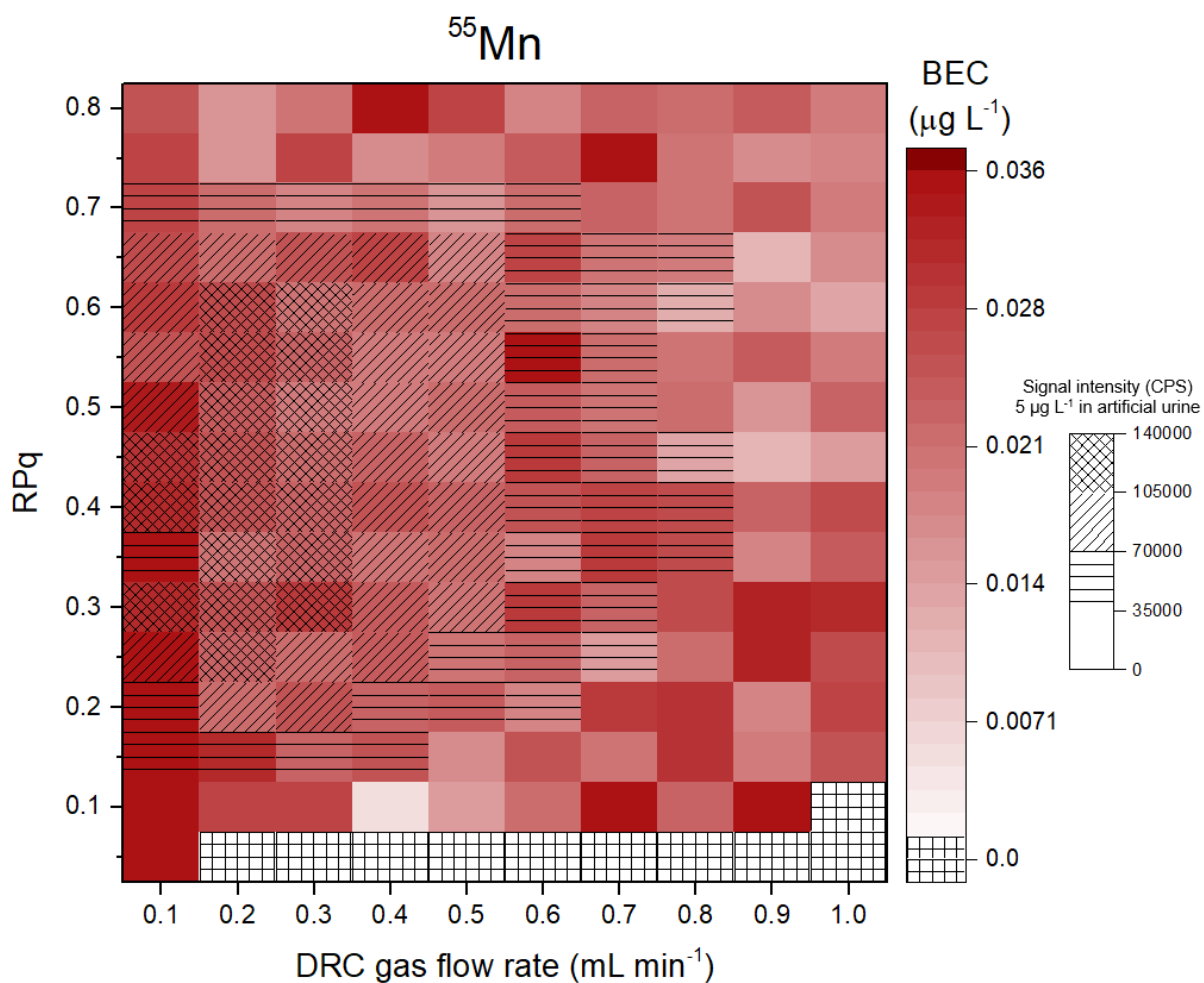


Fig. S.4 Results of DRC optimization (ammonia flow rate and RPq) in artificial urine spiked with  $5 \mu\text{g L}^{-1}$  of manganese. BEC represents a background equivalent concentrations of blank sample (unspiked artificial urine). Signal intensity (in CPS) measured for artificial urine spiked with  $5 \mu\text{g L}^{-1}$  of Mn is represented as textured rectangles in graph.

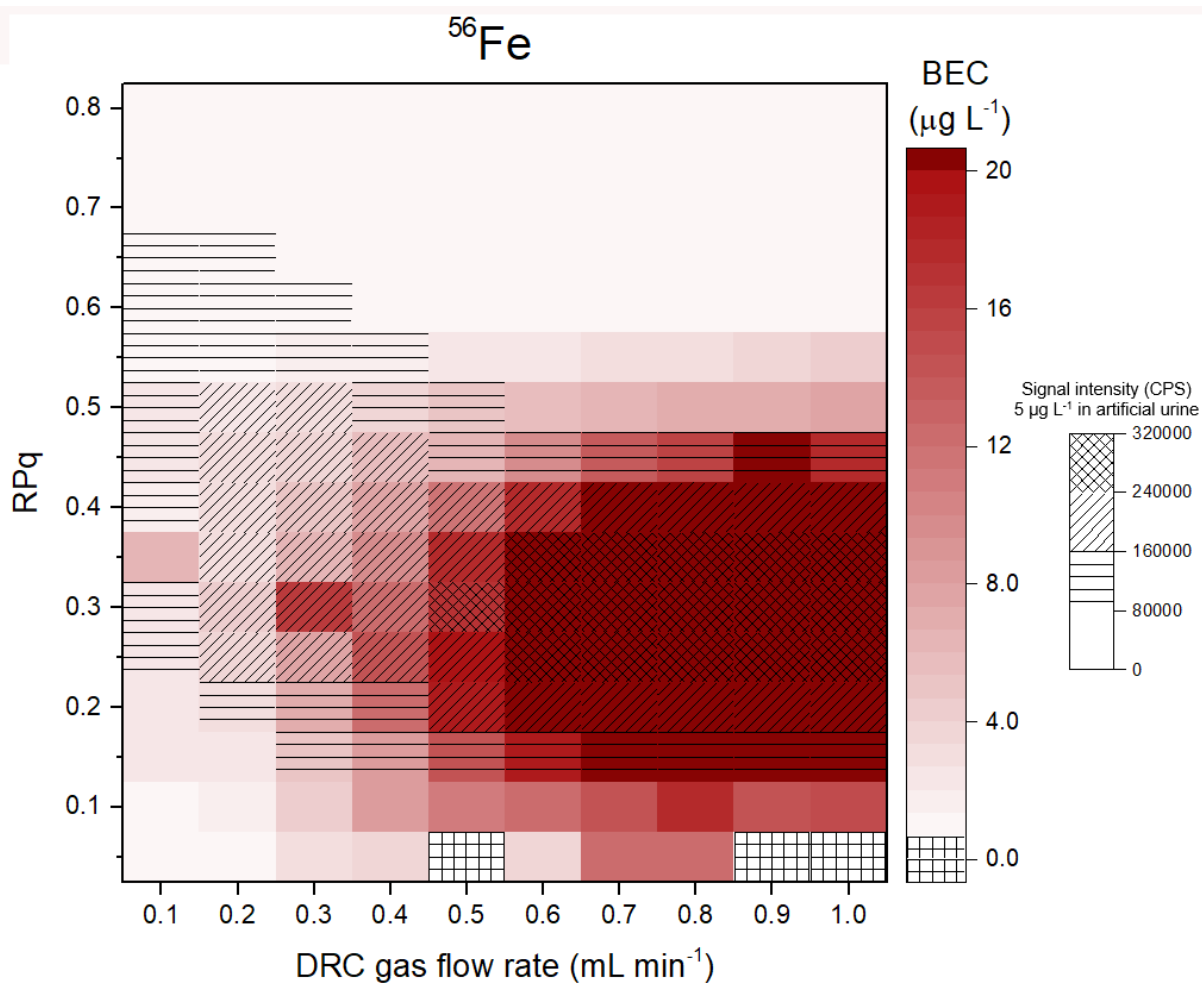


Fig. S.5 Results of DRC optimization (ammonia flow rate and RPq) in artificial urine spiked with 5  $\mu\text{g L}^{-1}$  of iron. BEC represents a background equivalent concentrations of blank sample (unspiked artificial urine). Signal intensity (in CPS) measured for artificial urine spiked with 5  $\mu\text{g L}^{-1}$  of Fe is represented as textured rectangles in graph.

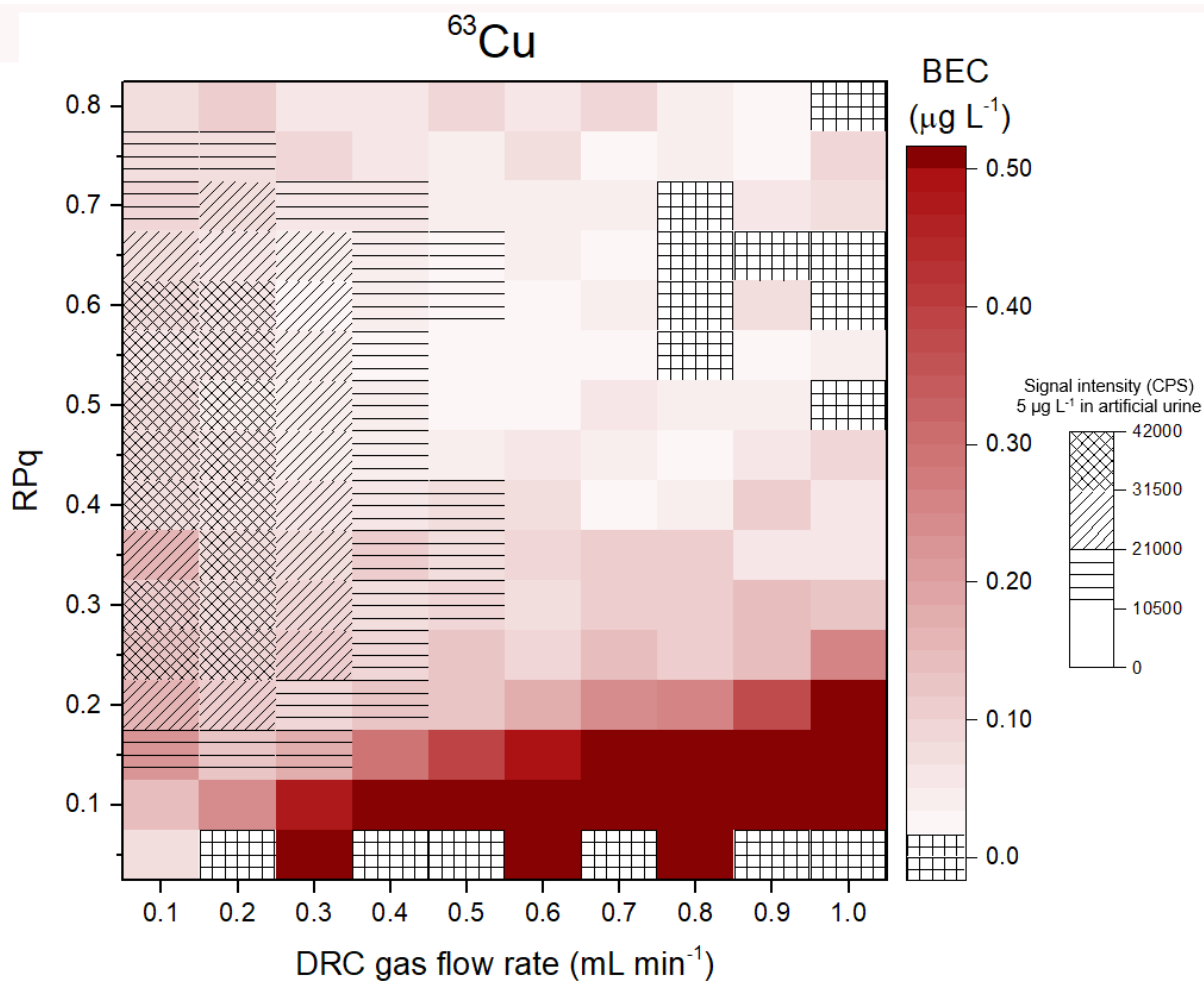


Fig. S.6 Results of DRC optimization (ammonia flow rate and RPq) in artificial urine spiked with 5  $\mu\text{g L}^{-1}$  of copper. BEC represents a background equivalent concentrations of blank sample (unspiked artificial urine). Signal intensity (in CPS) measured for artificial urine spiked with 5  $\mu\text{g L}^{-1}$  of Cu is represented as textured rectangles in graph.

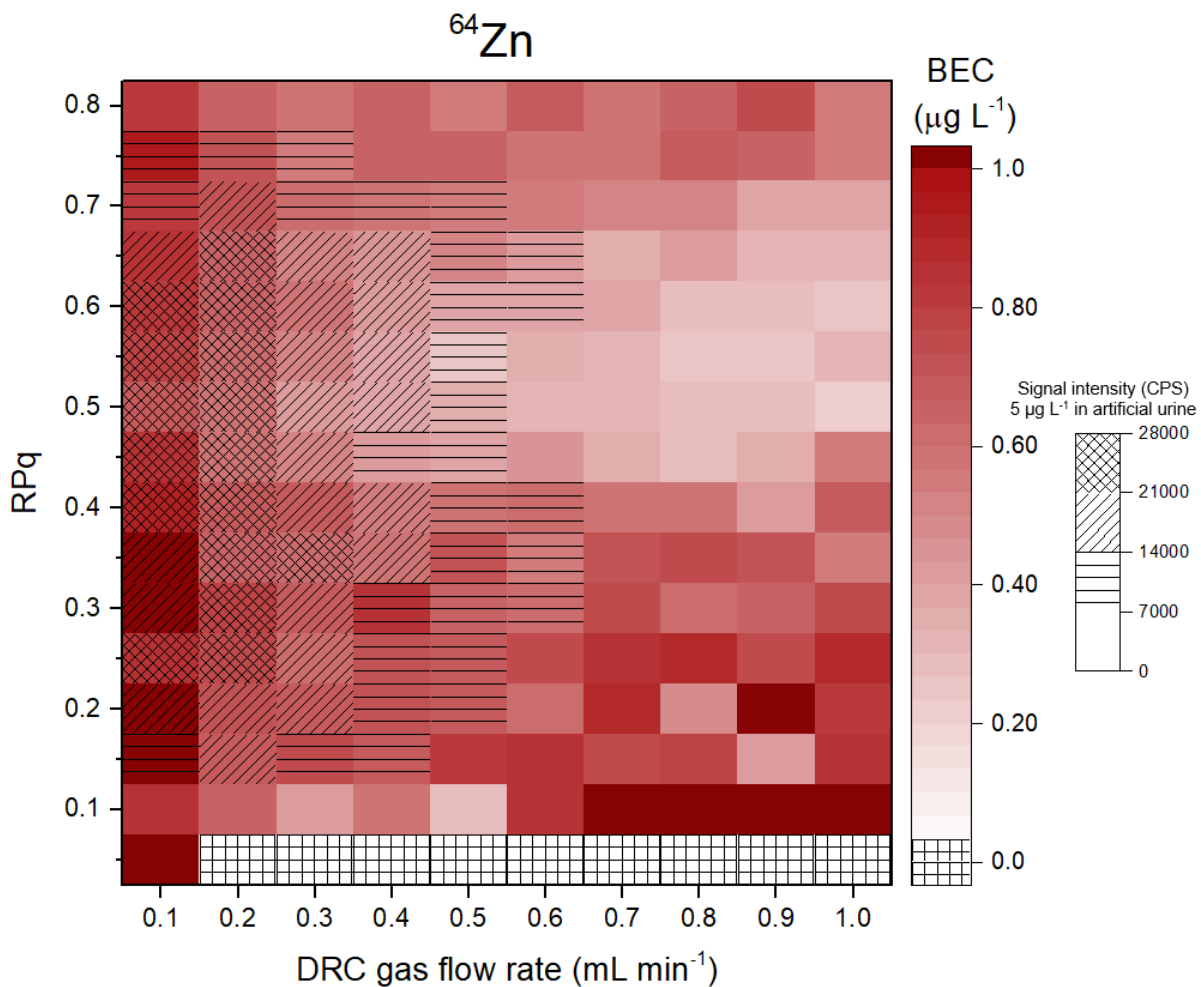


Fig. S.7 Results of DRC optimization (ammonia flow rate and RPq) in artificial urine spiked with  $5 \mu\text{g L}^{-1}$  of zinc. BEC represents a background equivalent concentrations of blank sample (unspiked artificial urine). Signal intensity (in CPS) measured for artificial urine spiked with  $5 \mu\text{g L}^{-1}$  of Zn is represented as textured rectangles in graph.

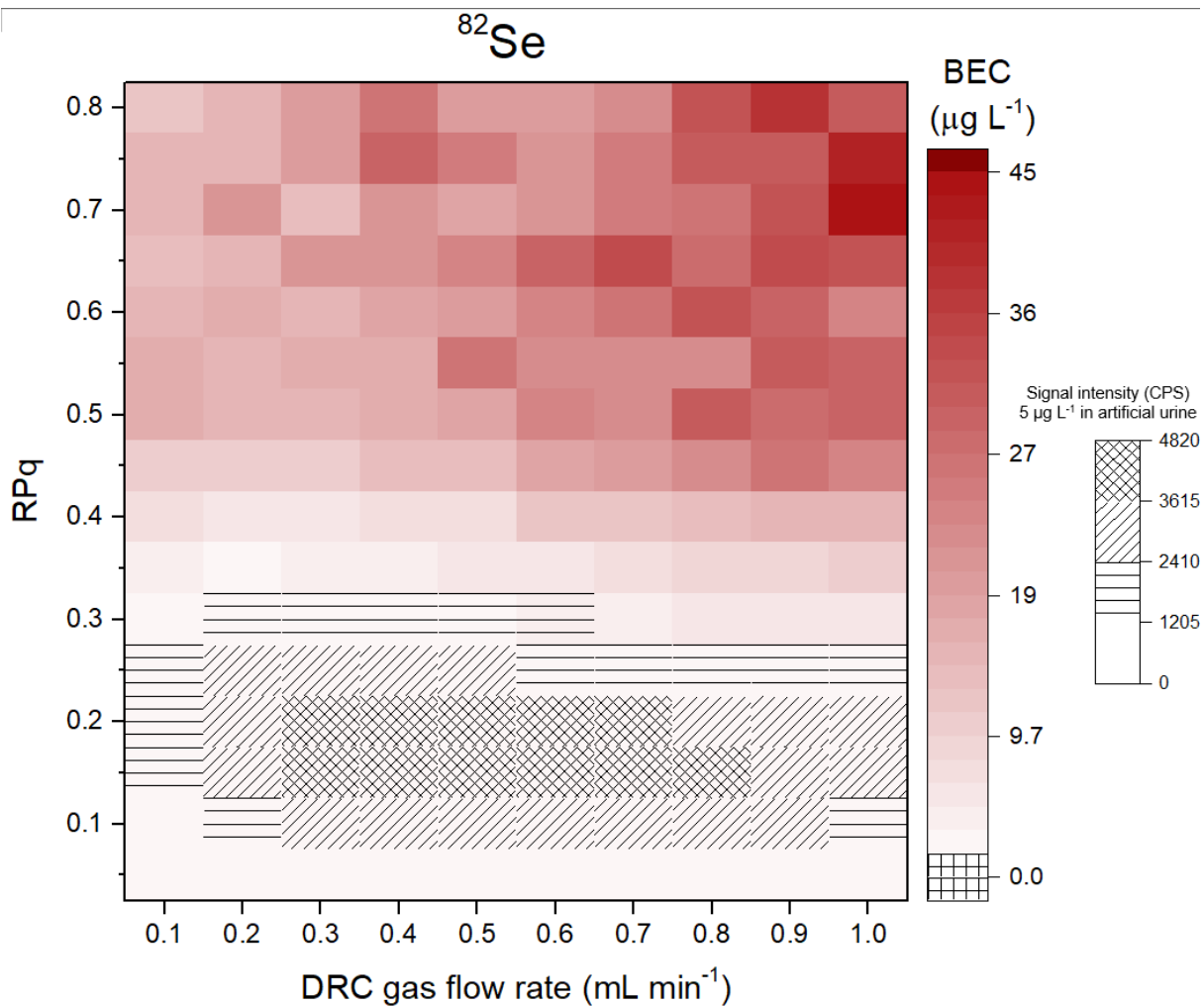


Fig. S.8 Results of DRC optimization (oxygen flow rate and RPq) in artificial urine spiked with  $5 \mu\text{g L}^{-1}$  of selenium. BEC represents a background equivalent concentrations of blank sample (unspiked artificial urine). Signal intensity (in CPS) measured for artificial urine spiked with  $5 \mu\text{g L}^{-1}$  of Se is represented as textured rectangles in graph.

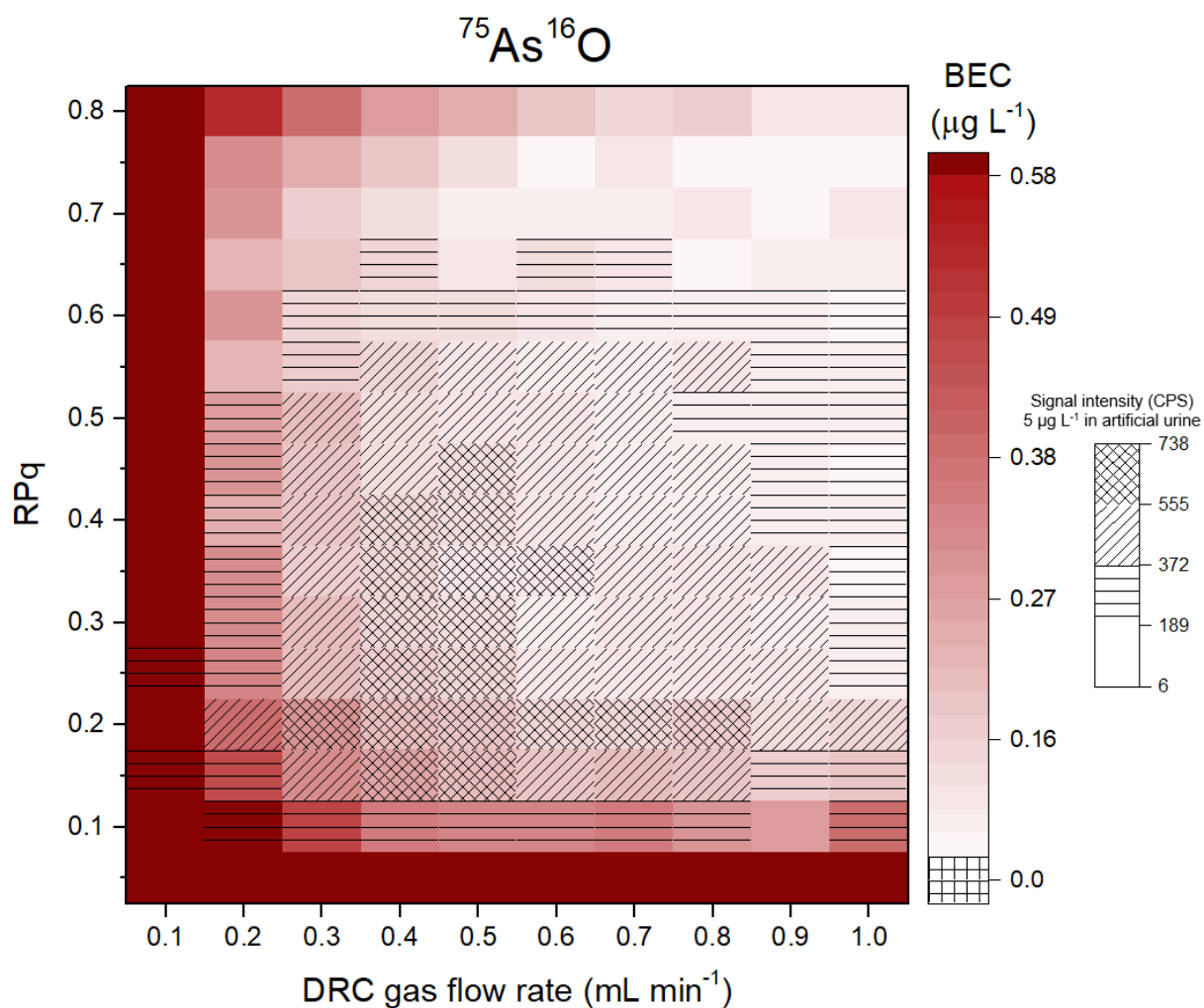


Fig. S.9 Results of DRC optimization (oxygen flow rate and RPq) in artificial urine spiked with  $5 \mu\text{g L}^{-1}$  of arsenic, measured as  $^{75}\text{As}^{16}\text{O}^+$ . BEC represents a background equivalent concentrations of blank sample (unspiked artificial urine). Signal intensity (in CPS) measured for artificial urine spiked with  $5 \mu\text{g L}^{-1}$  of As is represented as textured rectangles in graph.